Article ID: 1006-8775(2017) 04-0408-09

# ACCURACY OF THE RETRIEVED TEMPERATURE AND HUMIDITY FIELDS FOR TYPHOON HAIYAN UTILIZING THE ADVANCED TECHNOLOGY MICROWAVE SOUNDER

SHENG Wen-jie (盛文杰)[1], LIU Jian-wen (刘健文)[2] , HUANG Jiang-ping (黄江平)[2]
(1. PLA University of Science and Technology, Nanjing 211101 China;
2. Beijing Aviation Meteorological Institute, Beijing 100085 China)

**Abstract:** One-dimensional retrieval was performed on Typhoon Haiyan utilizing the advanced technology microwave sounder onboard the satellite Suomi NPP to retrieve the temperature and water vapor profiles of the typhoon. Comparisons of the retrieved profiles and ECMWF reanalysis were made to assess the results. The main conclusions are as follows. (1) The results have high spatial resolution and therefore can precisely represent the temperature and humidity distribution of the typhoon. (2) The retrieved temperature is low in the areas of low temperature and high in the areas of high temperature; similar patterns are observed for humidity. This means that systematic revision may be needed during routine application. (3) The results of the retrieved temperature and humidity profiles are generally accurate, which is quite important for typhoon monitoring.

**Key words:** 1-D VAR retrieving algorithm; temperature and humidity profiles; ATMS NPP; Typhoon Haiyan
**CLC number:** P 405 **Document code:** A
doi: 10.16555/j.1006-8775.2017.04.006

## 1 INTRODUCTION

The National Polar-Orbiting Operational Environmental Satellite System Preparatory Project (NPP) is an Earth environmental observation program jointly run by NASA, the National Oceanic and Atmospheric Administration (NOAA), and the US Air Force. The major satellite involved in this program at present is the Suomi NPP satellite (hereinafter NPP). The NPP satellite was launched on 27 October 2011 from Vandenberg Air Force Base, California, USA, the launch time window was 18:48—18:57 Beijing Time (BT) and the ascending node local time was 13:30. There were five sensors on board: the visible/infrared imager radiometer suite (VIIRS), cross-track infrared sounder, clouds and earth radiant energy system, advanced technology microwave sounder (ATMS), and ozone mapping and profiler suite, of which the ATMS is good at providing high-resolution air temperature and humidity parameters for both clear skies and cloudy and rainy weather. The scanning swath of the ATMS is a maximum of 2,500 km, 400 km wider than the Advanced Microwave Sensor Unit A (AMSUA) /microwave humidity sensor (MHS). The wider scanning swath allows a smaller gap between the satellite scanned bands, providing a much higher coverage rate of the earth. The higher coverage rate facilitates successive observations of weather systems and the wider scanning swath are better for imaging much larger scale weather systems more completely. There are 96 view points on every scan line of the ATMS, but only 30 and 90 on the AMSUA and MHS, respectively; thus, the scan points of the ATMS are denser than those of the AMSUA and the spatial resolution is correspondingly much higher.

One-dimensional variational (1-D VAR) retrieval (the 1-D VAR retrieving algorithm) is a recently developed physical retrieval method. The basic principle of the method is to establish the function relationship between atmospheric parameters and satellite observed brightness temperature via the atmospheric radiation transmission model and to reduce the difference between the simulated and observed brightness temperatures by gradually revising the atmospheric parameters from the initial profiles by iteration [1]. The advantages of this method are that its physical meaning is clear and definite and the retrieved results are believable. The 1-D VAR retrieving algorithm has a better physical basis and can essentially reflect nonlinear information better than those algorithms based on statistical methods, so theoretically, this method can be used unlimitedly throughout the day. Boukabara et al. applied this method for the global atmosphere and

**Received** 2016-05-13; **Revised** 2017-10-10; **Accepted** 2017-11-15
**Foundation item:** National Natural Science Foundation of China (91215302, 51278308); Open Project for State Key Laboratory of Atmospheric Boundary Layer Physics and Atmospheric Chemistry, Institute of Atmospheric Physics (LAPC)
**Biography:** SHENG Wen-jie, M.S., Assistant Engineer, primarily undertaking research on retrieval and utilization of satellite data.
**Corresponding author:** LIU Jian-wen, e-mail: liu_jianw@126.com

retrieved the total precipitable water under all weather conditions and underlying surfaces, and then compared the retrieved results with the analysis data of the global data assimilation system and ECMWF[2]. Comparison of the results proved that the retrieved temperature and water vapor profiles had a higher precision regardless of the weather conditions, although the accuracy of the retrieved cloud water path, total perceptible water, and other subgrade products were still poor due to the influence of water vapor. Liu et al. tested RTTOV and CRTM utilizing the atmosphere parameter output from WRF to compare the simulation capability of the two models in the case of a typhoon[3] . That study demonstrated that the varying scope of brightness temperature simulated by CRTM is larger than that simulated by RTTOV, but CRTM takes into account the scattering of four atmospheric components (cloud, rain, ice, and snow), which are incomplete in RTTOV. Dong et al. studied the multiple scattering effects of microwaves in typhoon systems and pointed out that with severe precipitation, the cloud and rain particles can give rise to stronger multiple scattering effects for microwave radiation, leading to a larger error in the simulated brightness temperature[4] . Forsthe et al. assimilated the AMSUA clear sky microwave detection data of NOAA-15 in January 2000 with the 1-D VAR retrieving algorithm, finding that 1-D VAR retrieval can improve the initial field of the numerical weather prediction model[5]. In addition, the 1-D VAR retrieving algorithm also possesses good adaptation to cloud-rain weather. This algorithm is characterized by better simulation of multiple scattering in cloud-rain areas due to the adoption of the CRTM radiation transfer model (Dong et al.[6]). The negative aspect of this method is that there are many matrix operations in the process, and it also involves incorporation of a forward radiative transfer operator, which requires high computational resources. In addition, the retrieval rigorously requires the accuracy of the initial field. In practice, the retrieval is restricted by the spatial-temporal matching error, typical error, and observation error between satellite data and observation data (Boukabara et al.[7]).

Typhoons are severe vortex structures generated over the northwest Pacific, which possess the distinctive characteristics of an eye and a spiral cloud band in shape, a downdraft in the center and updrafts in all the other parts of typhoons, and a warm core in the middle of the typhoon center. Typhoons are usually generated in the warm ocean of the western Pacific and thereafter move toward the northwest along with the easterly airflow on the south side of the subtropical anticyclone at 500 hPa, making landfall on South Asia and the southeast coastal regions of China. Typhoons are always accompanied by severe precipitation and extremely strong winds, so often cause huge damage on land. Therefore, investigating the inner structures, causes, and regular movement patterns of typhoons is good support for disaster prevention and mitigation. However, typhoons often occur in the ocean with powerful winds where observation sites are scarce, so it is difficult to perform conventional observations. Unlike conventional observations, satellites can monitor typhoons from space. Microwaves from the atmosphere can penetrate clouds and rain well, and the satellite multiple channels can provide maximum information on the atmosphere at different levels; thus, by using the polar orbit satellite to obtain observations and by using a certain retrieving algorithm, detection of the inner structures of typhoons can be improved.

In this study, we apply ATMS microwave data obtained during a typhoon to the 1-D VAR retrieving algorithm and compare the retrieved temperature and humidity profiles with the ECMWF reanalysis data to assess the retrieval accuracy of ATMS data. Section 2 contains a description of the data and retrieval methods used in this paper. The typhoon case study is introduced in Section 3. In Section 4, we describe the temperature and humidity profiles from ATMS data and compare the results with the ECMWF reanalysis data. A summary and conclusions are provided in Section 5.

## 2 DATA AND METHODS

### 2.1 *Data*

The Suomi NPP ATMS L1b data are stored in the HDF5 format. There are 22 channels in total, of which Channels 1—16 are designed to detect atmospheric temperature and 17—22 are for humidity. In the 16 temperature channels, relative to the AMSUA, Channel 4 is a new one with a central frequency of 51.76 GHz, and Channel 16 has had its central frequency adjusted to 88.2 Hz, which is based on the central frequency (89 GHz) of Channel 15 on the AMSUA. In the humidity-detecting channels, Channels 17 and 18 on the ATMS differ slightly in their central frequencies from Channels 2 and 3 on MHS, respectively. In the ATMS, the 89-GHz channel of MHS has been replaced by two new channels, Channels 19 and 21, which have frequencies of 183.31± 4.5 GHz and 183.31± 1.8 GHz, respectively, to enhance the sensing capability of water vapor and precipitation (Zou et al.[8]). The data utilized in this paper were collected around 0600 UTC 10 November 2013. This time period completely covered the typhoon zone, and so is able to reflect the morphology of the typhoon well.

ECMWF data were from the ERA-Interim reanalysis dataset, which was obtained through integrating satellite data, model prediction data, and conventional observation data from 1971 to the present using the 4D-VAR system (4-D variational data assimilation). The atmospheric parameters of the data are given on 37 pressure levels, and the times are at 0000, 0600, 1200, and 1800 UTC every day. This paper primarily uses the ERA-Interim reanalysis data of the global temperature and specific humidity fields at 0600

UTC on 10 November 2013. The horizontal resolution is 0.125° × 0.125°, and the vertical resolution is 37 pressure levels from 1,000 hPa to 1 hPa.

2.2 *1–D VAR retrieving algorithm*

The basic theory of the 1-D VAR retrieving algorithm is to use the to-be-retrieved atmospheric parameters, background field data, and satellite observation data to construct a cost function via the forward operator and then obtain the atmospheric parameters to be retrieved using the variational algorithm, minimizing the cost function (Boukabara et al. [1]). Mathematically, the algorithm is expressed as described below.

Suppose that $\mathbf{X}$ is the atmospheric parameter vector to be retrieved, $\mathbf{X}_0$ is the background field (the real values of the hypothetical atmospheric parameters), and $\mathbf{Y}^m$ is the brightness temperature of each channel in the satellite observations, then:

$$\min J(\mathbf{X})=[\frac{1}{2}(\mathbf{X}-\mathbf{X}_0)^T \times \mathbf{B}^{-1} \times (\mathbf{X}-\mathbf{X}_0)]+[\frac{1}{2}(\mathbf{Y}^m-\mathbf{Y}(\mathbf{X}))^T \times \mathbf{E}^{-1} \times (\mathbf{Y}^m-\mathbf{Y}(\mathbf{X}))] \quad (1)$$

where $\mathbf{B}$ is the background error covariance matrix, and $\mathbf{E}$ is the observation error covariance matrix.

$$\mathbf{B}_{n\_para\times n\_para}=\overline{(\mathbf{X}-\mathbf{X}_0)\times(\mathbf{X}-\mathbf{X}_0)^T} \quad (2)$$

$$\mathbf{E}_{n\_cha\times n\_cha}=\overline{(\mathbf{Y}^m-\mathbf{Y}(\mathbf{X}))\times(\mathbf{Y}^m-\mathbf{Y}(\mathbf{X}))^T} \quad (3)$$

where *n_para* is the length of the atmospheric parameter vector and *n_cha* is the number of channels. Thus, as long as the solution of one $\mathbf{X}$ is obtained, minimizing $J(\mathbf{X})$, then $\mathbf{X}$ is considered to be the retrieved atmospheric profile. So, when

$$\frac{\partial J(\mathbf{X})}{\mathbf{X}}=0 \quad (4)$$

the function $J(\mathbf{X})$ has its minimum value. Finally, the iterative formula is acquired:

$$\Delta\mathbf{X}_{n+1}=\left\{\mathbf{B}\mathbf{K}_n^T(\mathbf{K}_n\mathbf{B}\mathbf{K}_n^T+\mathbf{E})^{-1}\right\}\times\left[(\mathbf{Y}^m-\mathbf{Y}(\mathbf{X}_n)+\mathbf{K}_n\Delta\mathbf{X}_n\right] \quad (5)$$

where $\mathbf{K}$ is the Jacobian matrix of $\mathbf{Y}$ with respect to $\mathbf{X}$.

2.3 *Research steps*

Initially, the satellite data collected around 0600 UTC 10 November 2013 are divided into different domains to allow separate discussion and comparison of the different situations during the typhoon process. The typhoon (Domain a) is decomposed into three domains (Domain b, Domain c, and Domain d), which form three nonoverlapping subdomains within Domain a. Domain b lies in the southwest part of the typhoon spiral cloud band, and its underlying surface is land; Domain c is in the southeast part of the typhoon spiral cloud band, and its underlying surface is ocean; and Domain d is the Typhoon Eye. The Typhoon Eye is a relatively special domain in the typhoon structure, so it is treated as a separate domain in this paper. The specific latitude and longitude ranges of the four domains are depicted in Fig.1:

Domain a: 102—117 °E, 10—30 °N

Domain b: 105—107 °E, 14—17 °N

Domain c: 110—112 °E, 16—18 °N

Domain d: 109—110 °E, 18—19 °N

Subsequently, the results of the retrieved 500-hPa temperature and 850-hPa water vapor in Domain a are analyzed separately and compared with the ECMWF data. After that, the error distribution is analyzed. The two variables and their corresponding levels are selected because the temperature field at 500 hPa has significant

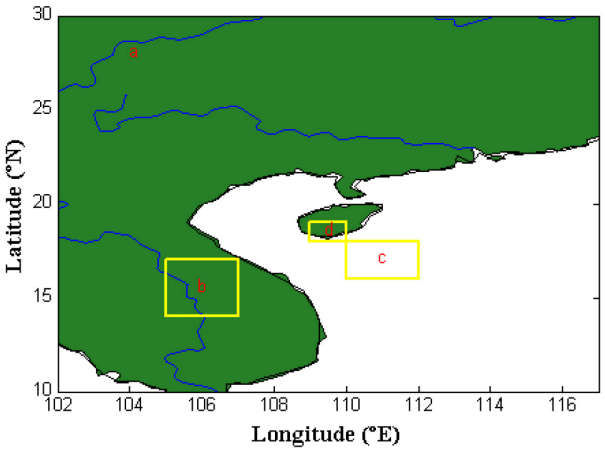


**Figure 1**. Division of the study region. (a) The overall typhoon area; (b) typhoon cloud- rain domain with land as the underlying surface; (c) typhoon cloud-rain domain with ocean as the underlying surface; (d) Typhoon Eye.

effects on the generation and development of mesoscale cyclones, while the humidity at 850 hPa is directly correlated to precipitation.

Finally, the temperature and humidity profiles of the three domains are compared with the reanalysis data, and then the average error profiles and root mean square error (RMSE) profiles are obtained. The average error profiles and RMSE profiles are calculated because the value of one point on the average error profile is the average of the difference between the retrieved data of this level in that typhoon domain and the reanalysis data. The average error profile is an overall reflection of the retrieval accuracy but cannot represent the proximity of the retrieval results and reanalysis data, whereas the RMSE can reflect this proximity much better. The smaller the value of the RMSE, the closer the retrieved result is to the actual data; conversely, the larger the value of RMSE, the greater the difference of the obtained result from the observation.

## 3 CASE STUDY

Typhoon Haiyan is used as a case study in this paper. This typhoon was generated over the northwest Pacific on 5 November 2013 and then moved northwest. On 7 November, it strengthened to a super typhoon and

moved closer to the Philippines. On the next day, it made landfall in the Philippines and thereafter directly moved toward China, landing in Hainan province on 10 November 2013. The typhoon caused serious loss of life and economic losses in the city of Sanya in the province. In its most powerful period, the maximum wind speed near its center was up to Grade 17 (75 m/s) or more, the lowest pressure in the center was 890 hPa (Yang et al.[9]).

Typhoon Haiyan arrived in Hainan around 0600 UTC 10 November 2013, when the NPP satellite was just passing over the area, so the typhoon was scanned by the satellite clearly and perfectly (Fig.2). In addition, because the strength of the typhoon was extremely powerful and the weather phenomena and atmospheric parameters were quite different from the ordinary situation, obviously typical characteristics were apparent, which is very helpful for testing the retrieval effect of the 1-D VAR retrieving algorithm. Thus, Typhoon Haiyan is ideal for retrieval case study.

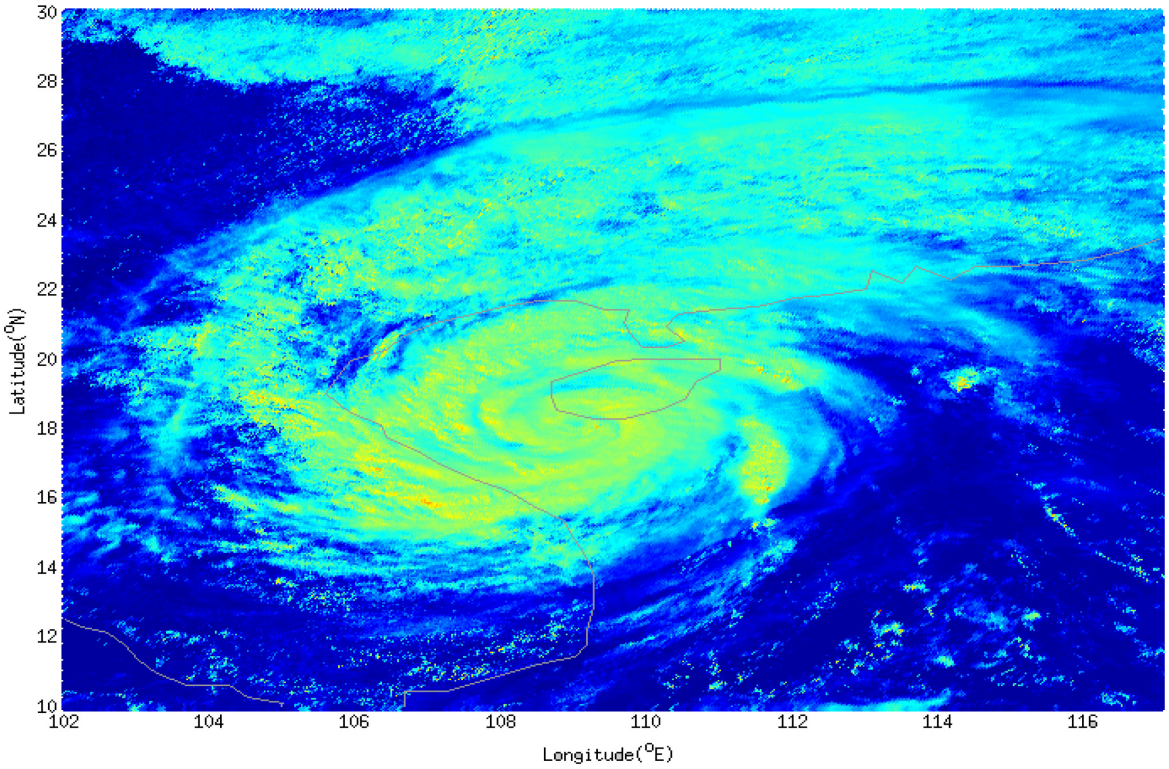


**Figure 2**. Satellite image of Typhoon Haiyan taken with NPP VIIRS.

## 4 RESULTS AND ANALYSIS

As the microwave channel was affected by the multiple-scattering effect of severe precipitation and cloud-rain particles, the retrieval result for the severe precipitation zone would have had sufficiently large errors such that the retrieval result could not be used. To measure such errors, the 1-D VAR retrieval system provides the spatial distribution of the $\chi^2$ value of the retrieval result. The $\chi^2$ value is defined as follows.

$$\chi^2 = \frac{1}{N}\left[(\mathbf{Y}^m - \mathbf{Y}(\mathbf{X}))^T \times \boldsymbol{B}^{-1} \times (\mathbf{Y}^m - \mathbf{Y}(\mathbf{X}))\right] \quad (6)$$

where $N$ is the number of channels, $\mathbf{Y}^m$ is the actual radiation values observed by all the channels of the satellite, $\mathbf{Y}(\mathbf{X})$ is the simulated result obtained by substituting the retrieval result $\mathbf{X}$ into the radiation transfer model, and $\boldsymbol{B}$ is the background error covariance matrix. Eq. (6) provides the covariance between the retrieval result of all the channels in a single view field and the actual observation data. If $\chi^2 \leqslant 5$, the retrieval result is reliable. The red zones in Fig.3 represent the $\chi^2 > 5$ situation, which means that the values of these zones are not believable. From Fig.3, the retrieval results of NPP are believable in most areas.

### 4.1 *Comparison of temperature fields*

#### 4.1.1 COMPARISON OF 500-hPa TEMPERATURES

Figure 4a shows that the retrieval results can display the detailed temperature field distribution diagram of typhoon at this level, due to the fairly high subsatellite point resolution. Comparison of Fig.4a and Fig.2 demonstrates that the temperature field can reflect the details of the spiral structure of the typhoon and the major cloud-rain band, but the typhoon diameter obtained by the retrieval is smaller than that observed. As illustrated in Fig. 4b, the retrieved temperature of the NPP microwave data is generally warmer by up to 10 K than the observed temperature on the spiral cloud-rain band of the typhoon; additionally, in the peripheral gale

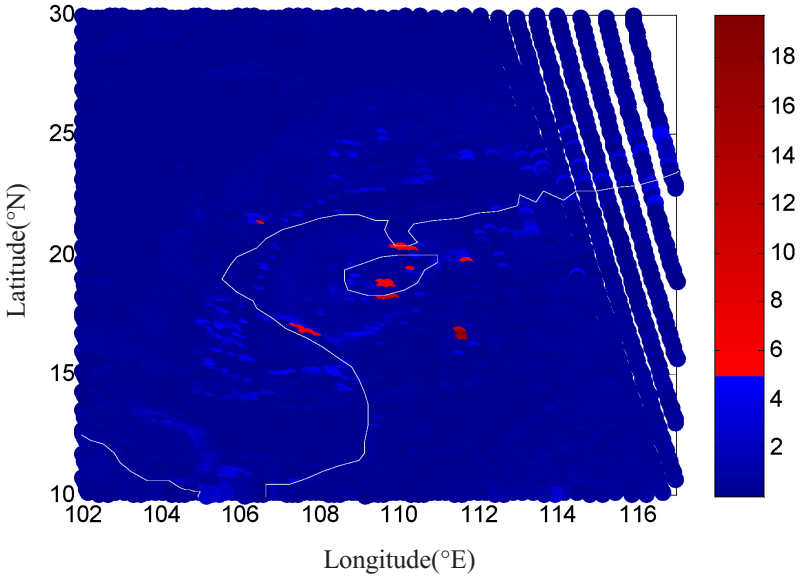


**Figure 3**. Distribution of $\chi^2$ values of the retrieval results.

zone the retrieval result of temperature is in general about 3 K higher. Fig.4c reveals the probability density distribution of errors: the average error retrieved by NPP is slightly bigger than 0, and the NPP errors are more concentrated; thus, the standard error is relatively small. Fig.4d shows a quantity-quantity diagram, in which the black line is the assembled molded line, the red line is the straight line obtained from the retrieval fitting results via the least-square method, and the colored bars on the right-hand side refer to the probability density distribution. The slope of the red line obtained from the NPP retrieval is smaller than 1; hence, for the actual low-temperature zone, the temperature retrieved is lower, whereas for the high-temperature zone, the retrieved temperature is higher.

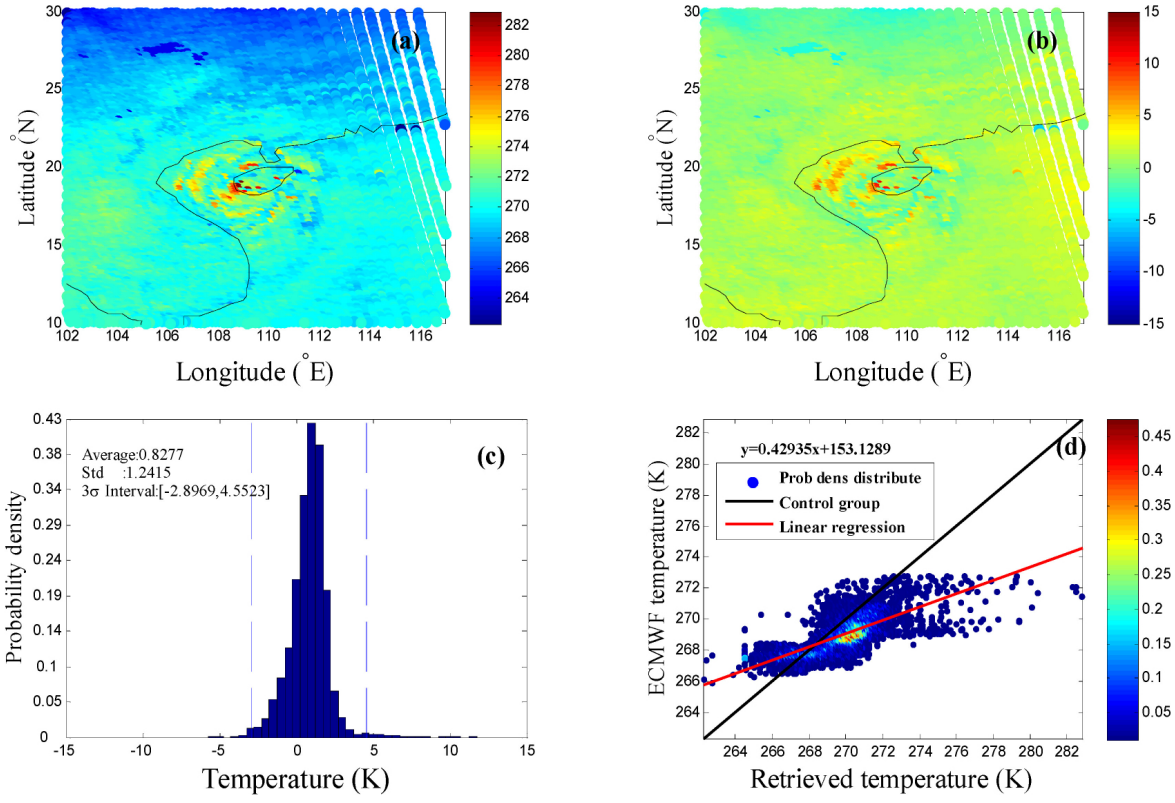


**Figure 4**. (a) NPP retrieved temperature (K) at 500 hPa, (b) differentials of the retrieval result and ECMWF reanalysis data, (c) probability density distribution histogram of differentials, (d) quantity-quantity plot of retrieval with respect to ECMWF.

#### 4.1.2 TEMPERATURE PROFILE RETRIEVAL

Figure 5a was obtained by averaging the differentials between the retrieval value of each domain in Fig.1 and the ECMWF reanalysis data. In general, in the near-surface levels larger errors are present in all the retrieved temperatures in the three domains; in the middle levels, such errors in the three domains are small and stable; and in the higher levels, the three errors fluctuate markedly. The overall retrieval error over the ocean surface below 900 hPa is smaller than that of the Typhoon Eye, and so the retrieval error is smaller than that over the land.

Figure 5b shows the retrieval accuracy of the three domains. The retrieval result is best for the area with land as the underlying surface, next best for the area with ocean as the underlying surface, and worst for the Typhoon Eye. Below 900 hPa, the temperature RMSE of land is about 1—2℃ and that of ocean is 2℃, but the value for the Typhoon Eye can be as much as 5—6℃. Between 800 hPa and 200 hPa, the temperature RMSE fluctuates near 1 K, the temperature RMSE over ocean is approximately 2℃, and the temperature RMSE in the Typhoon Eye can reach 3—5 ℃. These results for retrieval accuracy for land and sea are similar to the findings of Boukabara et al.[7].

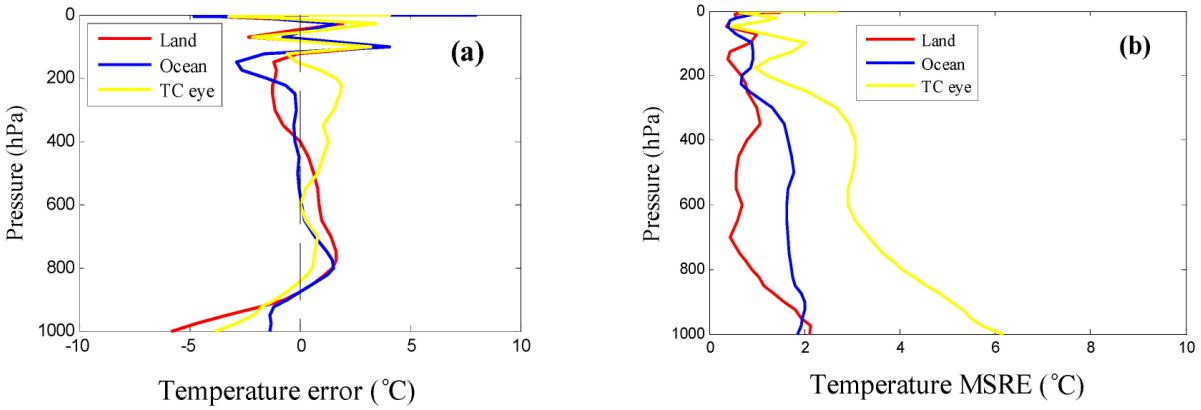


**Figure 5**. Profiles of (a) average temperature error and (b) RMSE.

### 4.2 *Comparison of humidity fields*

#### 4.2.1 COMPARISON OF 850-hPa HUMIDITIES

The layer where the water vapor of synoptic systems integrates is at 850 hPa. The vapor distribution and transmission of this layer is indicative for precipitation forecasting; thus, assessing the vapor retrieval of satellite data at 850 hPa under typhoon conditions is important. ATMS retrieval results (Fig.6a) can accurately reveal the detailed structure of the typhoon. The overall shape of the typhoon is similar to that illustrated in Fig.1. The minimum value zone of water vapor lies at 109°E, 19°N, and in its vicinity the spiral water vapor structure formed by the large-value zone is obvious. In the slightly peripheral area the typhoon clouds can be observed, with a water vapor content of approximately 15 g/kg. Fig.6b shows that for the spiral cloud-rain band, the retrieval error of water vapor is large, whereas for the area with smaller vapor content outside the spiral cloud-rain band the retrieval result is small. Fig.6c is the distribution of retrieval errors of water vapor. The average error is slightly smaller than 0, indicating that the overall retrieval value is small. In Fig.6d, the slope of the red line is less than 1, which means that for the area with higher observed vapor content the retrieval value is large, whereas in the area with lower observed vapor content, the retrieval value is small.

#### 4.2.2 HUMIDITY PROFILE RETRIEVAL

Figure 7a shows that the retrieved water vapor content in the Typhoon Eye below 800 hPa has positive errors, but the vapor content errors of land and ocean are mainly negative; at 800—400 hPa height, the error of water vapor content above the ocean is negative, whereas positive errors are apparent over land and in the Typhoon Eye, and above 400 hPa the retrieved vapor in the Typhoon Eye primarily displays positive errors. In Fig.7b, the accuracy of the retrieved vapor is similar to the temperature accuracy, i.e., best for land, second-best for ocean, and lowest for the Typhoon Eye, and the errors increase with decreasing height. In the higher levels, the retrieval errors are small, possibly because there is less water vapor in the upper air and there are fewer channels for the maximum information layer above 200 hPa. The RMSE of humidity increases with decreasing height. These phenomena are even more noticeable in the area of the Typhoon Eye. In the height below 850 hPa, the RMSEs of humidity for land, ocean, and the Typhoon Eye are approximately 1, 1.7, and 4—6 g/kg, respectively. Above 850 hPa, the RMSE over the land is stabilized at 1 g/kg or slightly smaller, the RMSE over the ocean decreases rapidly to 1 g/kg from 2 g/kg, and for the Typhoon Eye the RMSE is initially stable at 4 g/kg but later decreases rapidly. Beyond 300 hPa, the RMSEs for land, ocean, and the

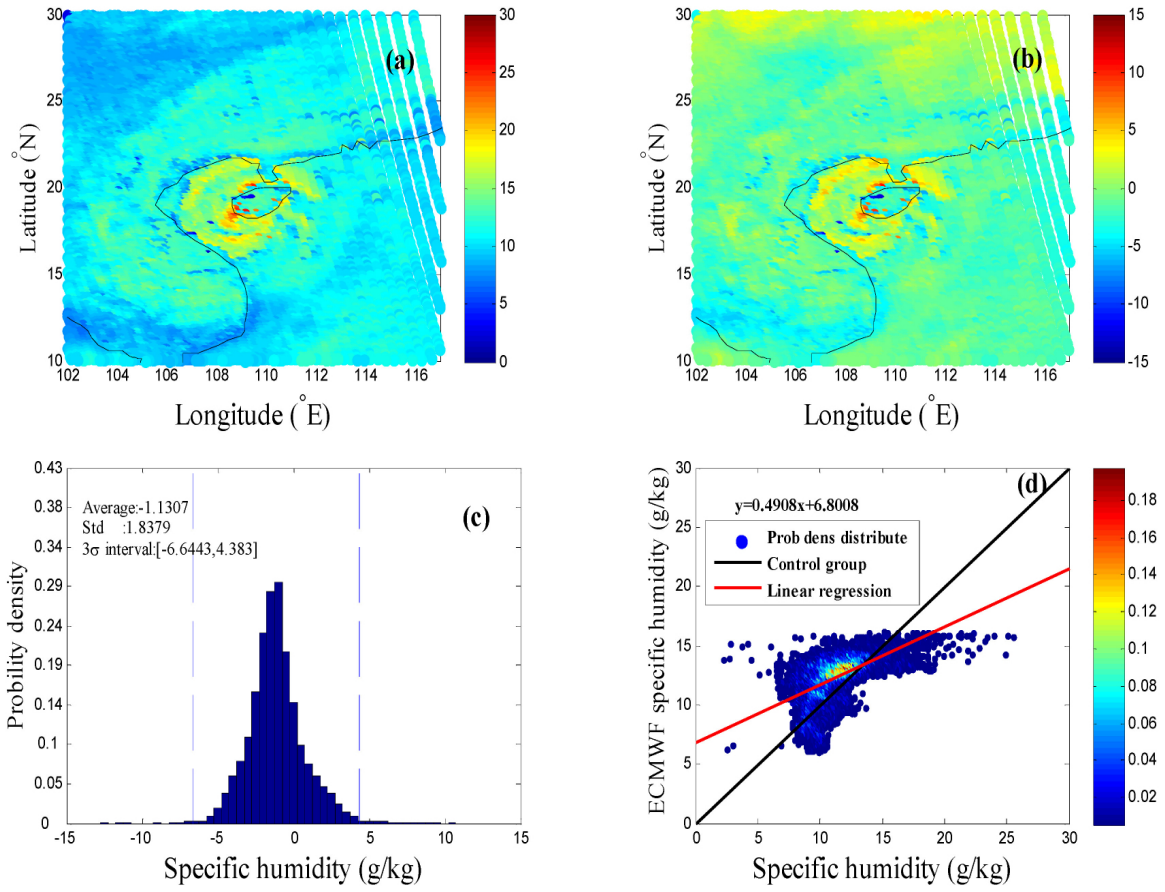


**Figure 6**. (a) NPP retrieved temperature at 850 hPa, (b) differentials of the retrieval result and ECMWF reanalysis data, (c) distribution histogram of differentials, (d) quantity-quantity diagram of retrieval result versus ECMWF reanalysis data.

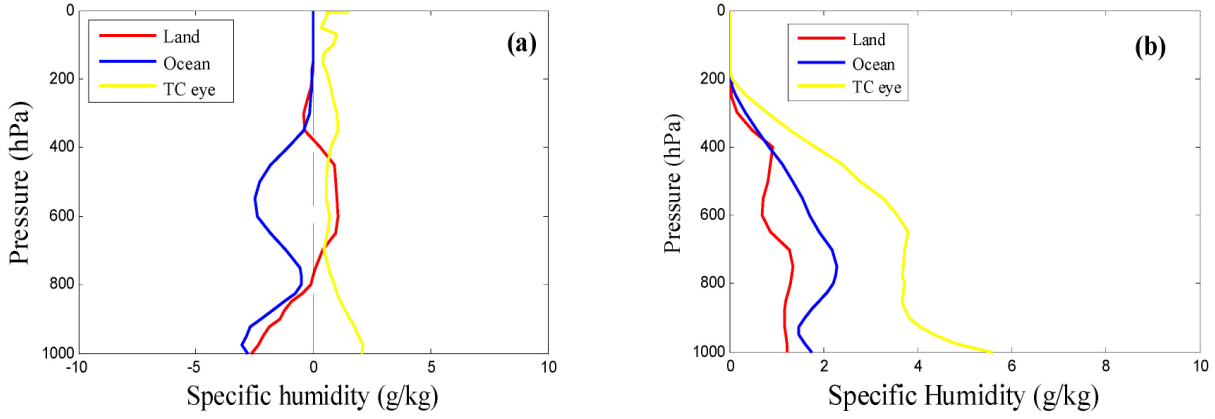


**Figure 7**. Profiles of (a) average humidity error and (b) RMSE.

Typhoon Eye are similar, all tending to be 0.

4.3 *Retrieval error analysis*

4.3.1 CAUSES OF THE LARGEST ERROR OF THE TYPHOON CENTER

The retrieval results described above demonstrated that the retrieval RMSE of the typhoon center is larger than the retrieval error of the spiral cloud band, which may be caused by the smaller scale of the typhoon center and the lower number of satellite observation points. Thus, when the scopes are limited in operation, the points of the eye wall are included in addition to the points of typhoon center. A problem is that the eye wall actually consists of very thick, towering convective clouds, thus creating greater errors.

4.3.2 SOURCES OF RETRIEVAL ERRORS

The slopes of the red lines (fitting line) in the

quantity-quantity diagram (Fig.4d and Fig.6d) are consistently less than 1. This result is attributed to the retrieval errors. In fact, the fitting line slope illustrates the highly nonlinear nature of the atmospheric radiation transfer model. Therefore, large errors are liable to be produced when solving problems reversely with the effect of either intensifying or weakening the atmospheric temperature and humidity fields. This can cause errors such that the retrieval results for the actual high-value atmospheric fields are much larger and the actual low-value atmospheric fields become even smaller, making the slope of the fitting line less than 1. In summary, the retrieval errors might be caused by several factors, as described below.

Although microwave radiation can penetrate the cloud-rain band well, the larger precipitation particles in the atmosphere still affect the transmission of microwaves. The retrieval errors in the present study might be caused by extinction effects of the severe precipitation and the thick clouds of typhoon on the microwave spectrum. Severe precipitation is an important factor that causes the retrieval to be more unstable.

The retrieval errors may also result from the errors of the initial field. The minimization method used in this paper is a gradient-descent method, which very easily converges to the local optimal solution. Accurate initial fields can both make the iteration converge faster and render it easier to converge to the global optimal solution; however, in the present study, we used the background as the initial field, which greatly deviates from the observations and thus the iteration is immersed in the local optimal solution, resulting in errors.

In addition, due to the design of the satellite, the atmospheric radiation transmission path is significantly lengthened when scanning the swath edge. Hence, even if the errors are corrected, the observational error is still present. For this reason, even if the retrieval model was absolutely accurate, it would still not be possible to obtain accurate atmospheric profiles.

## 5 CONCLUSIONS

Focusing on the case of Typhoon Haiyan, in this study we retrieved the temperature and humidity profiles by utilizing ATMS data. The retrieved zone was divided into three domains, and the profile average of the domains was obtained. Finally, the retrieval results and the ECMWF reanalysis data were compared. The conclusions are as follows.

The ATMS retrieved temperature and humidity profiles have higher spatial and temporal resolution than those retrieved by AMSUA. For every layer, the retrieval can reflect the distribution features of the typhoon in detail and can cover the typhoon area completely with high precision. This is very helpful for the location of the typhoon center, especially for an early-stage typhoon or a typhoon with weaker strength. In these cases, as the typhoon structure is not very noticeable or the spatial scale is too small, satellites with lower spatial resolution might fail to recognize the typhoon. Comparatively, the ATMS has higher spatial resolution and typhoon omissions are not likely to occur.

On the quantity-quantity diagram of retrieved temperature and water vapor, the slope of the best fit line (red line) is always smaller than 1, so the retrieval tends to exaggerate the actual weather systems. For the observed low-value area, the retrieval result shows an even lower value; for the observed higher value area the retrieval result shows an even higher value. Thus, this error should be corrected when applying this method in actual operations.

For the temperature and humidity profiles in different domains, the RMSE gradually decreases with increasing height. At heights above 850 hPa, the temperature RMSE is less than 1 ℃ over the land, less than 2 ℃ over the ocean, and less than 5 ℃ over the Typhoon Eye; the humidity RMSE is less than 1 g/kg over the land, less than 2 g/kg over the ocean, and less than 4 g/kg over the typhoon Eye. This finding suggests the retrieval results of NPP for the typhoon are in good agreement with the actual observations.

The 1-D VAR retrieving algorithm used in this paper does not require special parameter setting to the retrieving algorithm for a specific case; thus, this retrieving algorithm can be applied in other typhoon cases without changing any of the parameters. This is of great importance for practical temperature and humidity profile retrieval of typhoons. It should be mentioned, however, that the background field is taken as the iterative initial field in this paper. More accurate initial fields will be used in future experiments, such as NWP or sounding observation data. In this study, we analyzed the case of Typhoon Haiyan, but the 1-D VAR retrieving algorithm can also be used to analyze large-scale weather processes in the mid-high latitudes, such as frontal cyclones, Meiyu weather, and rainstorm processes. Further work using this method will be carried out in the future.

**REFERENCES:**

[1] BOUKABARA S A, GARRETT K, CHEN W, et al. MiRS: An all-weather 1DVAR satellite data assimilation and retrieval system [J]. IEEE Trans Geosci Remote Sens, 2011, 49(9): 3249-3272.

[2] BOUKABARA S A, GARRETT K, CHEN W. Global coverage of total precipitable water using a microwave variational algorithm [J]. IEEE Trans Geosci Remote Sens, 2010, 48(10): 3608-3621.

[3] LIU Shuo-song, DONG Pei-ming, HAN Wei, et al., Simulation study and comparison of satellite microwave observation to Typhoon Krosa by RTTOV and CRTM [J]. Acta Meteor Sinica, 2012, 70(3): 585-597 (in Chinese).

[4] DONG Pei-ming, LI Wei, HUANG Jiang-ping, et al., The effect of moisture variables on satellite microwave remote

sensing and its sensitivity analysis [J]. Remote Sens Technol Appl, 2014, 29(2): 300-308 (in Chinese).
[5] FORSTHE J M, KIDDER S Q, JONES A S, et al., Moisture profile retrievals from satellite microwave sounders for water analysis over land and ocean [J]. J Atmos Ocean Technol, 2001, 18(3): 345-352.
[6] DONG Pei-ming, WANG Hai-jun, HAN Wei, et al. Effect of water substance on the simulation of cloud zone satellite microwave observation [J]. J Appl Meteor Sci, 2009, 20 (6): 682-691 (in Chinese).
[7] BOUKABARA S A, GARRETT K, GRASSOTTI C, et al. A physical approach for a simultaneous retrieval of sounding, surface, hydrometeor, and cryospheric parameters from SNPP/ATMS [J]. J Geophys Res Atmos, 2013, 118(22): 12600-12619.
[8] ZOU X, WENG F, LIN L, et al. Impacts of assimilation of ATMS data in HWRF on track and intensity forecasts of 2012 four landfall hurricanes [J]. J Geophys Res Atmos, 2013, 118(20): 11558-11576.
[9] YING M, ZHANG W, YU H, et al. An Overview of the China Meteorological Administration Tropical Cyclone Database [J]. J Atmos Ocean Technol, 2014, 31 (2): 287-301.

**Citation:** SHENG Wen-jie, LIU Jian-wen and HUANG Jiang-ping. Accuracy of the retrieved temperature and humidity fields for Typhoon Haiyan utilizing the advanced technology microwave sounder [J]. J Trop Meteor, 2017, 23(4): 408-416.